THREE-DIMENSIONAL OPEN-CELLULAR MATERIALS FORMED FROM SELF-PROPAGATING POLYMER WAVEGUIDES

Alan J. Jacobsen [1], William Barvosa-Carter[1], Steven Nutt [2]
[1] *Sensors and Materials Laboratory, HRL Laboratories, LLC, Malibu, CA 90265 (USA)*
[2] *Gill Foundation Composites Center, University of Southern California, Los Angeles, CA 90089 (USA)*

ABSTRACT

Composite sandwich structures rely on lightweight core materials of sufficient thickness to separate two rigid facesheets. Cellular materials that have closed-cell configurations are commonly used as cores for sandwich structures, and include materials such as honeycomb with a two-dimensional ordered structure or polymer foams with a three-dimensional random cellular configuration. Recently a new type of cellular material has been developed that may be useful for sandwich structure cores. This new cellular material is formed from an interconnected three-dimensional pattern self-propagating photopolymer waveguides. The technique of patterning self-propagating polymer waveguides can rapidly form thick open-cellular materials, and the resulting microstructure of these materials has a three-dimensional truss architecture and sub-millimeter features. In addition, the truss configuration can be easily tailored using this fabrication technique, enabling the mechanical properties of the cellular material to be designed for specific applications.

1. INTRODUCTION

Cellular materials, which are materials with significant porosity, have considerably lower bulk density than their solid counterparts, and thus are ideal as cores for sandwich structures. However, at the cost of reducing the mass of a material by introducing porosity, mechanical properties such as the strength and elastic modulus are significantly diminished. Ordered cellular structures generally exhibit an increase in modulus and peak strength relative to random cellular configurations by changing the mode of deformation from bending-dominated to stretch/compression-dominated within the microstructure during elastic loading [1]. Nevertheless, techniques to fabricate three-dimensional ordered open-cellular materials, particularly with feature sizes ranging from tens to hundred of microns, are limited. Recently, a new technique to produce cellular materials with micro-scale truss structures from a three-dimensional interconnected pattern of self-propagating polymer waveguides was developed [2]. A two-dimensional schematic representation of this process is shown in Figure 1.

Example polymer micro-truss structures that can be formed using this process are shown in Figures 2 and 3. These structures are formed by exposing a two-dimensional mask with a pattern of circular apertures that is covering an appropriate photomonomer. Within the photomonomer, polymer waveguides originate at each aperture in the approximate direction of the UV collimated beam and polymerize together at points of intersection. The points of intersection are the nodes of the three-dimensional truss structure. In addition, the self-propagating phenomenon enables rapid formation of thick (> 5 mm) three-dimensional open-cellular polymer truss structures. The samples shown in Fig. 2 had an exposure time of less than one minute. A more detailed description of this process can be found in reference [2].

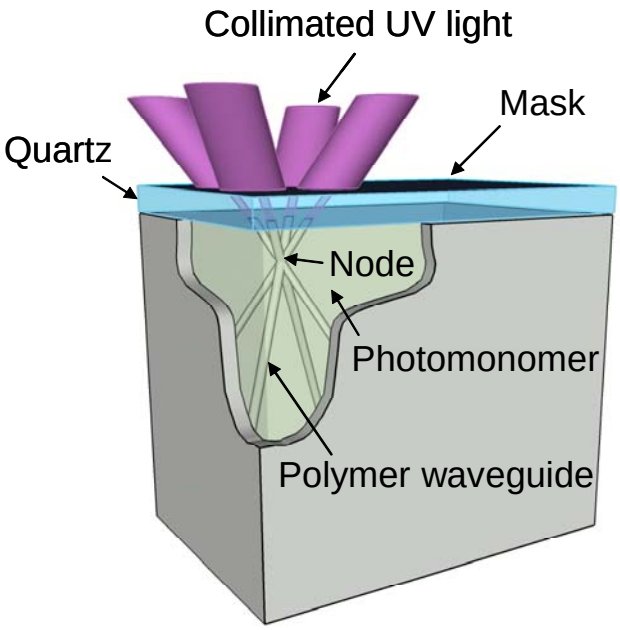

Figure 1: Schematic representation of the process used to from micro-truss structure from a self-propagating polymer waveguides [2]. *Reprinted with permission.*

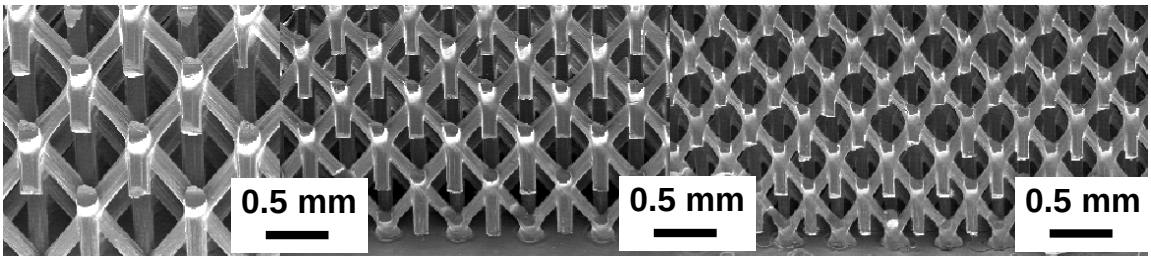

Figure 2: SEM images of polymer three-dimensional truss materials with different waveguide diameter and spacing.

In Figure 2, the unit cell architecture and waveguide (or truss-member) angle is the same between samples, but the size-scale is different. These variations are possible by changing aperture spacing and diameter on the mask. The flexibility of the process also enables variations in waveguide (truss-member) angle and unit cell architecture. By controlling these parameters, the mechanical properties of the core material can vary considerably [3,4], enabling sandwich structure cores to be designed for specific applications.

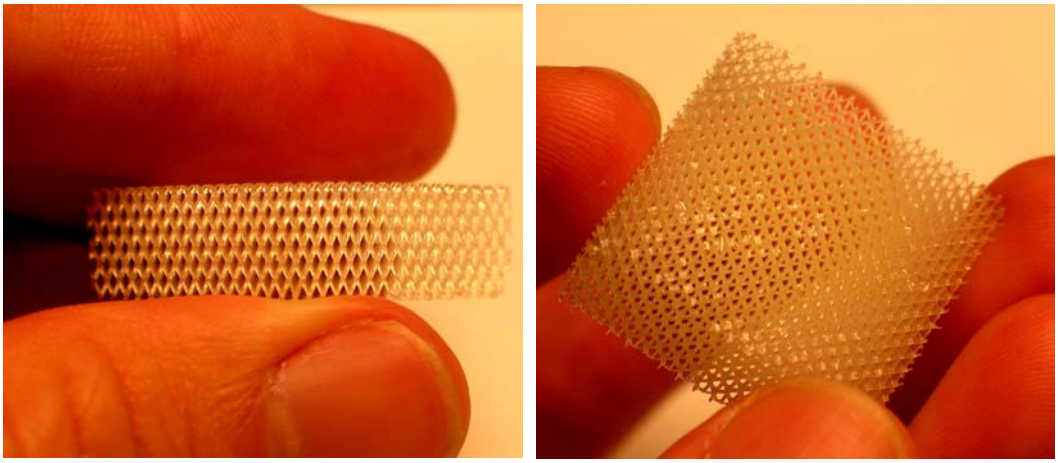

Figure 3: Thick samples of the three-dimensional polymer truss materials.

2. ANALYTICAL PREDICTION OF MECHANICAL PROERTIES

All the micro-truss structures discussed in this paper had an octahedral-type repeating unit cell shown in Figure 4. This representative unit cell is fabricated by exposing a mask with a square pattern of circular apertures to four collimated beams with the same incident angle but rotated 90° apart with respect to the mask normal, as shown in Figure 1. Because of the uniform truss microstructure, simple analytical equations can be derived to predict the compressive and shear properties of these cellular materials.

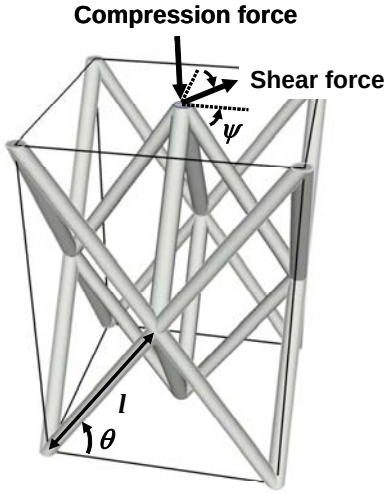

Figure 4: Representative unit cell of the micro-truss structures.

2.1 Compression

An analytical expression to predict the compressive modulus of the micro-truss structures can be derived by conducting a work (energy) balance on the unit cell shown

in Figure 4, assuming the initial strain of the bulk micro-truss structure is transferred as pure axial strain to the truss members (with pinned end constraints). Eqn. (1) is the relationship to predict the compressive modulus (E) based on the modulus of the solid material (E_s), the angle of the waveguides (or truss members) relative to the plane normal to the compressive load (θ), and the relative density, which is the density of the cellular material (ρ) divided by the density of the solid polymer from which its comprised (ρ_s) [3,5]. Eqn. (2) is a similar relationship for the compressive strength of the micro-truss structure, which was derived by a simple force balance.

Compressive modulus: $$E = E_s \sin^4\theta\,(\rho/\rho_s) \quad (1)$$

Peak compressive strength: $$\sigma = \sigma_s \sin^2\theta\,(\rho/\rho_s) \quad (2)$$

The peak compressive strength of the micro-truss structures is a function of the peak strength of the individual truss members (σ_s), which ultimately depends on their slenderness ratio [3, 5]. Long slender truss members, when loaded under compression, will fail by elastic, or Euler buckling. For the polymer micro-truss structures considered in this work, elastic buckling should occur when slenderness ratio of the truss members, which is defined as truss member length (l) divided by truss member radius (r), is greater than approximately 25. For micro-truss structures fabricated with truss member slenderness ratios between approximately 5 and 25, the truss members should fail by inelastic buckling when loaded in compression. Micro-truss structures with truss members that have a slenderness ratio less than approximately 5 should fail by material yielding.

2.2. Shear

Through a similar analytical approach, the expressions shown in Eqs. 3 and 4 can be derived to predict the shear modulus (G) and peak shear strength (τ_p) of these micro-truss structures [4,5].

Shear modulus: $$G = \frac{E}{8}(\sin^2 2\theta)(\rho/\rho_s) \quad (3)$$

Peak shear strength: $$\tau_p = \frac{\sigma_p}{4}\frac{\sin 2\theta}{\cos\psi}(\rho/\rho_s) \quad (4)$$

While the effective shear modulus is independent of the shear force direction (ψ), the shear strength of the octahedral-type unit cell is periodic in ψ, with the minimum shear strength occurring at $\psi = 0°$ and the maximum occurring at $\psi = 45°$ [4,5]. Also, the peak shear strength is a function of the peak failure strength of the individual truss members (σ_p). Since a shear load on these micro-truss structures, as defined in Figure 4, will lead to truss members in both tension and compression, the failure strength will be dependent on both the buckling behavior of the truss members in compression and tensile yielding (or fracture) behavior of the truss members in tension.

3. EXPERIMENTAL RESULTS

Compression and shear loading experiments have been conducted on various micro-truss samples with different waveguide (or truss member) diameter, length, and angle. These parameters affect the resulting relative density of the micro-truss structures, which as shown in Section 2, is directly proportional to the modulus and strength of the micro-truss structures in both compression and shear. Section 3.1 summarizes the compression experiments described in detail in reference [3] and Section 3.2 summarizes the shear experiments described in detail in reference [4].

3.1 Compression

Quasi-static compression tests were conducted on five different polymer micro-truss samples. The relative density and approximate waveguide angle of the five samples is listed in Table 1. The micro-truss samples were sandwiched between quartz faceplates prior to compression testing. The faceplates were attached to the compression surfaces of the samples with a thin layer of the same photopolymer used to fabricate the samples. The faceplates constrained the nodes at the compression surfaces, enabling axial deformation of the truss members during early stages of compression, as shown in Figure 5.

Table 1: Summary of the key sample parameters and measured and predicted properties for samples tested under compression.

Sample	Relative Density, ρ/ρ_s (%)	Approximate Waveguide Angle, θ (deg)	Compression Modulus, E (MPa)		Peak Strength, σ_p (MPa)	
			Predicted	Measured	Predicted	Measured
1	13.5	59 ± 1.2	173	152 ± 0.7	6.0	2.9
2	16.2	59 ± 1.2	209	182 ± 1.1	7.3	3.5
3	12.7	51 ± 0.8	110	96 ± 1.0	4.7	1.6
4	13.8	51 ± 0.8	120	103 ± 0.6	5.2	2.2
5	12	59 ± 0.6	155	123 ± 0.5	5.2	2.3

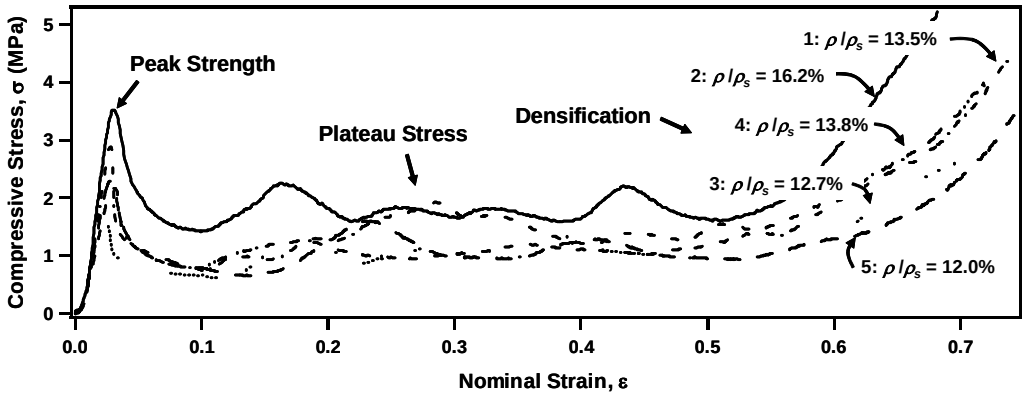

Figure 5: Compressive stress-strain response of the polymer micro-truss samples [3].

The increase in compressive stress eventually caused the truss members in each sample to buckle. The maximum stress carried by each sample at buckling was defined as the peak strength of the sample. The misalignment of the buckled truss members caused bending-dominated behaviour (rather than axial-compression-dominated behaviour) of the truss members during subsequent compressive loading, leading to a relatively constant plateau stress. Eventually the micro-truss samples reached their respective densification strain, which was dependent on the relative density of the sample.

In Table 1, the measured compression modulus and peak strength of each sample is compared to the respective predicted values calculated from Eqns. (1) and (2). The compressive modulus of the solid polymer (E_s) used to fabricate the micro-truss samples was 2.4 GPa. The peak buckling strength of the individual truss members (σ_s) was calculated from the compression strength of the solid polymer and their respective slenderness ratios using inelastic buckling theory [6].

The predicted modulus of these micro-truss samples compares well with the measured values; however, the predicted peak strength of the micro-truss samples is significantly greater than the measured values. This discrepancy in the measured and predicted values has been attributed to microstructural imperfections and the nonlinear (viscoelastic) behavior of the polymer, as discussed in reference [3].

3.2 Shear

The single-lap shear experiments on the micro-truss samples were conducted following ASTM standards. A total of nine micro-truss samples were fabricated and tested under these shear conditions, as discussed in [4]; however, in this paper we are highlighting two samples that represent the spectrum of data collected. As with the compression samples, the shear surfaces were bonded to quartz faceplates to constrain the nodes. The samples were then bonded to the steel shear test fixture plates with an acrylic adhesive, as shown in Figure 6.

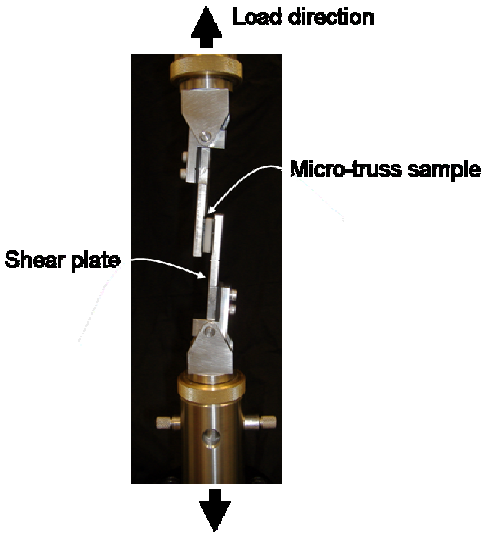

Figure 6: Single-lap shear fixture used to test polymer micro-truss samples.

Table 2 includes the relative density, approximate waveguide angle, and the shear force direction (see Figure 4) for the two shear samples. The nominal shear stress-stain curves for these samples are shown in Figure 7.

Table 2: Summary of the key sample parameters and measured and predicted properties for samples tested under shear.

Sample	Relative Density, ρ/ρ_s (%)	Approximate Waveguide Angle, θ (deg)	Shear Force Direction ψ (deg)	Shear Modulus, G (MPa)		Measured Peak Shear Strength, τ_p (MPa)
				Predicted	Measured	
5	12.5	51 ± 0.8	0	34	19 ± 0.1	0.9
6	15.4	59 ± 1.2	45	35	34 ± 0.3	1.5

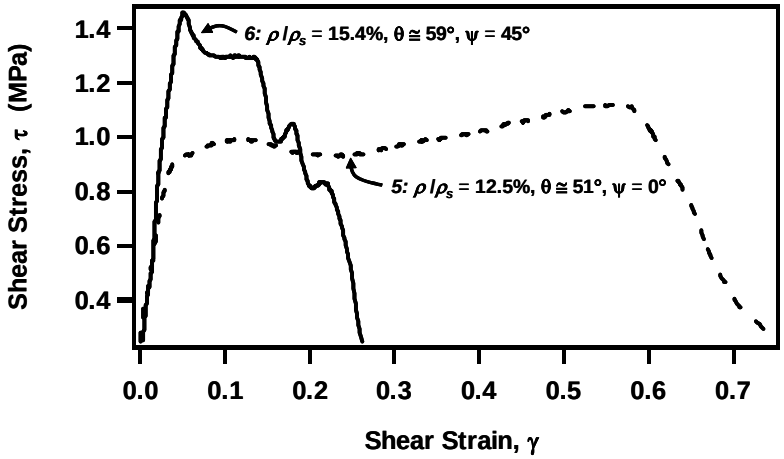

Figure 7: Shear stress-strain response of two polymer micro-truss samples.

The measured shear modulus G for each sample was determined from the average slope of the respective nominal shear stress-strain curve during elastic loading, and the predicted shear modulus was calculated using Eqn. (3). For Sample 6, the predicted modulus is within 3% of the measure value; however, there is a considerable difference in these predicted and measured values for Sample 5. The discrepancy between the measured and predicted shear modulus for Sample 5 was attributed to three factors: 1) the lower relative density of the sample, 2) the reduced truss member angle in comparison to Sample 6, and 3) the shear force direction.

Micro-truss samples with a lower relative density become more susceptible to non-ideal deformation, such as truss member bending and twisting, during shear loading conditions. This increases the deviation from the idealized prediction, which assumes only axial strain in the truss members.

For micro-truss samples with a reduced truss member angle ($\theta \cong 51°$ in comparison to $\theta \cong 59°$), the polymer waveguides that form the truss members have to propagate farther for a fixed sample thickness. Through observation of sample micrographs, micro-truss

structures with $\theta \cong 51°$ generally have additional structural defects, such as initial truss member curvature and/or misalignment, which will also reduce the measured modulus.

As described in Section 2.2, the shear modulus should be independent of the shear load direction. However, when the shear force is applied in the direction corresponding to $\psi = 0°$, nearly all the load is carried by only half of the truss members. This indicates that the actual maximum stress in the truss members carrying a given shear load is greatest when $\psi = 0°$. For a shear force in the direction $\psi = 45°$, the applied shear load is distributed more uniformly between all truss members for the unit cell configuration shown in Figure 4. The imperfections in the structure previously described, coupled with the non-uniform distribution of load associated with a shear load direction $\psi = 0°$, will lead to an additional reduction in measured shear modulus.

An analytical prediction of the peak shear strength of the polymer micro-truss structures is more complicated than predicting the shear modulus. This is because there are competing mechanisms that will cause initial failure of the truss members. These competing mechanisms include material yielding for the truss members under tension and buckling for the truss members under compression. In addition, the micro-truss structures have fixed nodes and thus can carry moments. This will lead to a complex state of stress in the truss members, particularly for a shear load direction $\psi = 45°$.

As shown in Figure 8a and 8b, the shear failure response of a polymer micro-truss sample is also related to the distribution of failure through the thickness of the sample. Figure 7 shows that Samples 5 and 6 display distinct behavior after their respective peak shear strength. This large plateau shear strain for Sample 5 is attributed to the uniform distribution of failure through the thickness of the structure. Although Sample 6 had greater peak shear strength, this sample exhibited much less plateau shear strain because the failure was localized in a single unit cell layer. Further studies are necessary to better understand the conditions which lead these different distributions of failure through the polymer micro-truss structures.

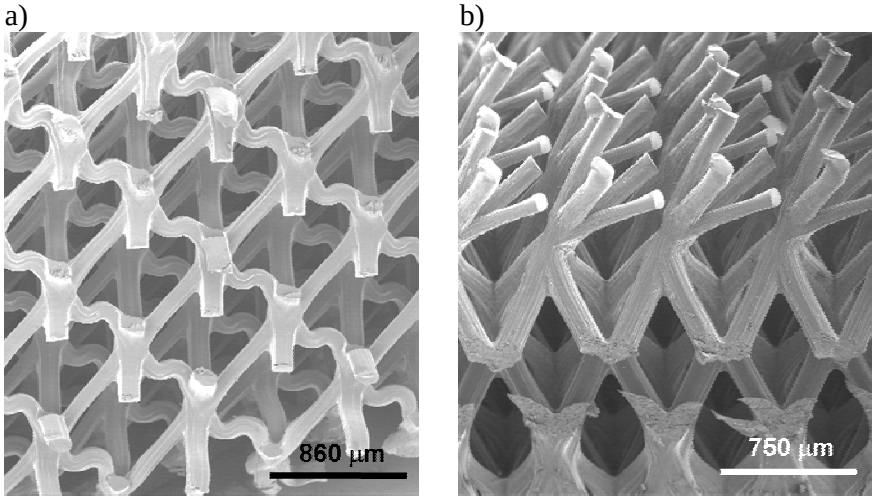

Figure 8: Micrographs of a) Sample 4 and b) Sample 5 after shear loading [4].

4. CONCLUSIONS

In this paper we have summarized our recent work on the fabrication and mechanical characterization of micro-truss structures formed from an interconnected three-dimensional pattern of self-propagating photopolymer waveguides. This technique can create a variety of open-cellular micro-truss structures with controlled mechanical properties that may be used as cores for composite sandwich structures. In contrast to foams with a random cellular configuration, the truss architecture of these materials enables the use of simple analytical models to predict the mechanical properties. These materials also can provide a specific strength and specific stiffness enhancement over random cellular materials by suppressing the bending-dominated behaviour in the microstructure during mechanical loading. In addition, the open-cellular nature of these polymer micro-truss structures allows for possible multifunctional applications that are prohibited with commonly used sandwich structure cores, such as honeycomb and closed-cellular foams.

ACKNOWLEDGMENTS

One of the authors (A J Jacobsen) would like to thank the National Physical Science Consortium for fellowship support. Also, the authors thank Chaoyin Zhou and Bob Doty for their helpful discussions and technical assistance.

REFERENCES

1. Ashby, M. F., "The properties of foams and lattices." *Phil. Trans. R. Soc. A*, Vol. 364, pp 15-30, 2006.
2. Jacobsen A.J., Barvosa-Carter W. and Nutt S., “Micro-scale truss structures formed from self-propagating photopolymer waveguides.” *Advanced Materials*, 2007;19:3892–3896.
3. Jacobsen A.J., Barvosa-Carter W. and Nutt S., “Compression behavior of micro-scale truss structures formed from self-propagating polymer waveguides.” *Acta Materialia*, 2007;55:6724–6733.
4. Jacobsen A.J., Barvosa-Carter W. and Nutt S., “Shear behavior of micro-scale truss structures formed from self-propagating polymer waveguides.” *Acta Materialia*, 2008;56:1209–1218.
5. Deshpande V.S., and Fleck N.A, “Collapse of truss core sandwich beams in 3-point bending.” *Int. J. Solids Struct*, 2001;38:6275-6305.
6. Gere J.M. and Timoshenko S.P., “Mechanics of Materials.” 1984, Monterey, CA: Wadsworth, Inc.